



Semnan University

# Progress in Engineering Thermodynamics and Kinetics Journal

Journal homepage: <https://jpetk.semnan.ac.ir/>



## Research Article

# Nitrate adsorption from synthetic aqueous solutions by $\text{Ca}(\text{OH})_2$ and Clinoptilolite zeolite nano-particles

Faezeh Ghodrati <sup>a</sup>, Azadeh Hemmati <sup>b\*</sup>, Morteza Faghihi <sup>c</sup>, Ziba Ashrafi <sup>a</sup>,

<sup>a</sup> Department of Petroleum and Chemical Engineering, Islamic Azad University, Science and Research Branch, 1477893855, Tehran, Iran

<sup>b</sup> Department of Chemical, Petroleum, and Gas Engineering, Semnan University, 3513119111, Semnan, Iran

<sup>c</sup> Chemistry & Process Engineering Department, Niroo Research Institute, 1468613113, Tehran, Iran

## ARTICLE INFO

### Article history:

Received: 202\*-\*\*-\*\*

Revised: 202\*-\*\*-\*\*

Accepted: 202\*-\*\*-\*\*

### Keywords:

Adsorption;

Nitrate;

$\text{Ca}(\text{OH})_2$ ;

Zeolite;

Nano-particles.

## ABSTRACT

In this research article, the authors utilized a ball mill to grind Clinoptilolite zeolite 98% and  $\text{Ca}(\text{OH})_2$  nanoparticles, and subsequently characterized the resulting adsorbents using SEM, TEM, XRD, and FTIR analyses. To optimize the adsorption process, they employed the Box-Behnken Design (BBD) of Response Surface Methodology (RSM) to evaluate the impact of various parameters, including pH (ranging from 5 to 9), adsorbent amount (ranging from 0.5 to 2 g), and temperature (ranging from 25 to 45 °C). The authors determined that the optimal temperature for nitrate adsorption was 45°C at a pH of 5, using 2g of adsorbent. Applying the pseudo-second-order dynamic model for investigation, the optimal retention time was determined to be 15 min. The maximum amounts of nitrate removed by  $\text{Ca}(\text{OH})_2$  and zeolite were found to be 60.34% and 58.04%, respectively, with the the absorption equilibrium equation fitting well to the Langmuir model. Under optimal conditions, a mixture of  $\text{Ca}(\text{OH})_2$  and zeolite (at a ratio of 1:3) removed a maximum of 56.70% of nitrates. These findings demonstrate the significant potential of natural zeolite and  $\text{Ca}(\text{OH})_2$  for nitrate adsorption.

© 2024 The Author(s). Progress in Engineering Thermodynamics and Kinetics Journal published by Semnan University Press.

## 1. Introduction

Access to underground water is crucial for human survival in many parts of the world. However, the growing global population and rising demand for agricultural and industrial products have

\* Corresponding author.

E-mail address: [Azadehemmati@semnan.ac.ir](mailto:Azadehemmati@semnan.ac.ir)

Cite this article as:

Ghodrati, F., Hemmati, A., Faghihi, M., & Ashrafi, Z. (2024). Nitrate adsorption from synthetic aqueous solutions by  $\text{Ca}(\text{OH})_2$  and Clinoptilolite zeolite nano-particles. *Progress in Engineering Thermodynamics and Kinetics*.

<https://doi.org/10.22075/JPETK.2023.24860.1004>

resulted in increased levels of nitrate compounds - such as nitrogen and ammonia - penetrating water sources [1-6]. This trend poses a significant threat to both humans and the environment, as excessive nitrate contamination of groundwater can lead to the conversion of nitrate to the nitrite form, which increases the risk of cancer and causes the blue baby syndrome in infants [2-4, 7-9]. To address this issue, the World Health Organization (WHO) and US Environmental Protection Agency (EPA) have established guidelines specifying the maximum acceptable levels of nitrate in drinking water as 10 mg/L and 50mg/L, respectively [8, 10-14].

Nitrate contamination of water resources has become a major concern in today's world. The primary sources of nitrate contamination in groundwater include industrial and agricultural wastewater, fertilizers, and septic systems [15]. Researchers have proposed several methods for removing or reducing nitrate in water, including the utilization of ion exchange resin, as well as both biological and chemical denitrification methods. electro-dialysis, osmosis reversal, and adsorption [10, 11, 13, 15]. Among these methods, the adsorption process is currently considered the most cost-effective and efficient way to remove harmful pollutants from contaminated water [13, 14]. Various samples of adsorbents have been studied, including activated carbon [16-18], clay minerals [19, 20], alumina, biomaterials, zeolites [21], and others [22]. Despite the high cost of activated carbon, it is still widely used due to its effectiveness in removing pollutants [23].

Zeolite is a commonly found natural sorbent that is cost-effective and an excellent alternative to other expensive adsorbents. The high potential of zeolites for ion adsorption, ion exchange, and molecular screening can be attributed to their unique properties. Zeolites come in various types, with differences in purity, crystal size distribution, and chemical composition [24-29]. They are hydrated alumina-silicate minerals with porous and spherical shapes and are composed of three-dimensional grids of  $\text{SiO}_4$  and  $\text{AlO}_4$  tetrahedra, with oxygen atoms being common among them. Replacing some of the cations such as  $\text{Si}^+$  and  $\text{Al}^+$  with  $\text{Na}^+$ ,  $\text{K}^+$ , and  $\text{Ca}^{2+}$  in zeolites can reduce the negative charge in their overall chemical structure [30-36].

The properties of zeolites that affect their adsorption capabilities include their chemical and structural composition, the Si/Al ratio, the type of cation, and the number and location of cavities. The behavior of zeolites in the adsorption process also depends on the shape, ion size, the density of the anionic framework, ionic charge, and the concentration of the solution of the external electrolyte. Various parameters, such as pH, contact time, and cationic surfactants, can impact the adsorption properties of zeolites [37-40].

Clinoptilolite is the most prevalent zeolite in the natural world and exists in vast quantities [36]. The structure of zeolites comprises open channels of 8-10 rings [41-43], with other types of zeolites including mordenite, phillipsite, chabazite, stilbite, and analcime and laumontite.

Advanced English: Applications of calcium hydroxide include the protection of cultural heritage, medical usages, steel industry, building materials and adsorbents for a variety of colours. Calcium hydroxide has been used as a useful and cost-effective adsorbent to remove indigo carmine dye in wastewater. Calcium hydroxide is environmentally friendly and the risks are manageable [44-46] Calcium hydroxide is a low-cost adsorbent and widely found in nature [44].

Previous studies have investigated the removal of nitrate by various micro sized-adsorbents. But the nano-materials are being studied by researchers in the field of water and wastewater treatment due to the high surface area and reactivity of them [47, 48]. Some researchers have done research on nitrate removal using zeolite. Onyango and his coworkers prepared functionalized zeolite to remove nitrate from water [49]. They found that with increase in adsorbent dosage, the percentage removal of nitrate was raised. In addition, functionalized zeolite showed efficient nitrate adsorption in wide range of temperature and pH without a significant change in performance. Schick et al. used a surfactant to modify zeolite for nitrate removal from aqueous solution [37]. They reported the good adsorption of modified zeolite and declared that this adsorbent is potentially applicable to separate nitrate contamination in surface or ground waters. Similar results in nitrate removal using modified zeolite have been reported in the research of Guan et al. [50]. They noted that different zeolite nitrate removal performance can be due to amounts of surfactant loadings and the source of zeolite supply. Research on nitrate separation by raw or modified zeolite has been discussed in the literature, but nitrate removal by calcium hydroxide ( $\text{Ca}(\text{OH})_2$ ) has received less attention. Hernandez et al. used aqueous carbonation of calcium hydroxide to remove nitrate [51]. They claimed the nitrate exhibited no physicochemical affinity while calcite was forming.. Examination of the literature indicates that the study on the separation of nitrate by calcium hydroxide can still be investigated. So in this work, the nitrate removal using zeolite and  $\text{Ca}(\text{OH})_2$  are studied.

In order to model and design experiments, one useful method is Response Surface Methodology (RSM), which is a useful tool for determining the optimal parameters in a process [52, 53]. In this research, In order to maximize nitrate adsorption effectiveness by adsorption under various operating circumstances, Box-Behnken was utilized.

The study used  $\text{Ca}(\text{OH})_2$  and Clinoptilolite zeolite nanoparticles as the adsorbent for nitrate adsorption. Additionally, kinetic and isotherm models were used to forecast the zeolite and

Ca(OH)<sub>2</sub> nanoparticles' adsorption capabilities. Furthermore, the effects of different experimental conditions, such as the pH and temperature of the adsorbent, were investigated using RSM modeling.

## 2. Materials and Methods

### 2.1. Reagents and Solutions

In this research, the clinoptilolite used was obtained from the Semnan mine. Nitrate lead salt, hydrochloric acid, Ca(OH)<sub>2</sub> (Merck, Germany), and double distilled water were utilized. Nylon membrane filter with a diameter of 25 mm and a pore size of 0.2 μm was acquired from Vertical, located in Thailand.

### 2.2. Preparation of Zeolite and Ca(OH)<sub>2</sub> Nano-particles

The preparation of nano-particles was carried out using sieving and milling methods [54, 55]. Analytical T90 sieves were employed to separate particles of zeolite and Ca(OH)<sub>2</sub> that were smaller than 0.01 microns. The nano-particles of zeolite and Ca(OH)<sub>2</sub> were then using Mechanical processes and a Planetary milling machine (with a speed of 300 Revolutions per minute for 20 hours). Finally, the zeolite prepared e and Ca(OH)<sub>2</sub> nanoparticles were stored in desiccators to prevent moisture absorption.

### 2.3. Nitrate adsorption

Initially, A solution measuring three liters in volume of nitrate with a concentration of 20 mg/l in Double-refined water was prepared. The adsorption tests were conducted via the mixture of appropriate volumes of zeolite and Ca(OH)<sub>2</sub> nanoparticles mixing in 50 ml of the nitrate solution. The pH was tuned to the desired levels by adding 0.1 and NaOH at a concentration of 1 M or 0.1 and 1mol/L HCl liquid mixtures. For each run, a certain measure of sorbent was mixed with 50 milliliters of the nitrate solution and agitated at 250 rpm for a duration of 30 minutes at room temperature. In the next step, the solution was separated from the adsorbent using a centrifuge (Napco R2028) at 8000 rpm for 20 minutes. The amount of nitrate adsorption was measured using a spectrophotometer (DR5000 Hach) with the standard method book. Every measurement was repeated three times, and the average of the results was reported. The percent amount of nitrate adsorption was calculated using The following mathematical expression:

$$\text{Removal percentage} = 100 \times (C_i - C_{eq}) / C_i \quad (1)$$

in which  $C_i$  and  $C_{eq}$  are the starting and equilibrium concentrations of nitrate in each solution (mg/L), respectively.

## 2.4. Analytical Methods

The purity and mineralogical composition of zeolite and  $\text{Ca}(\text{OH})_2$  were determined by a Seifert PTS 3003 X-ray diffractometer. A planetary mill was used to prepare  $\text{Ca}(\text{OH})_2$  and zeolites nano-particles. A planetary ball mill (Retsch PM100 model Germany) was used to prepare  $\text{Ca}(\text{OH})_2$  and zeolites nano-particles. In order to determine the molecular structure in terms of spectroscopy, the Fourier transformation-infrared spectra (FT-IR) (Nexus 780 model, America) was used. Nano-particle size and morphology of nanoparticles were measured by Transmission Electron Microscope (TEM) (Philips EM208). The surface morphology of the nano-particles of zeolite and  $\text{Ca}(\text{OH})_2$  before and after the adsorption of nitrate were studied by Scanning Electron Microscopy (SEM)(Philips 8010).

The concentration of nitrate solutions was measured by a UV-Vis spectrophotometer (HACH DR5000, Germany) based on standard methods provided by HACH The pH of the liquids was measured using a Swiss Metrohm pH meter.

## 2.5. Experimental Design

To investigate the effect of the aforementioned parameters on nitrate adsorption using zeolite and  $\text{Ca}(\text{OH})_2$  nanoparticles and optimize each factor, experiments were designed using a surface response method in a box-banner design with Mini Bar software (Version 17). Three independent variables were used, including pH, to investigate their impact on the reaction rate (5, 7, and 9), Degree of heat (25, 35, and 45 °C), and the quantity of sorbent (0.5, 1.25, and 2 g). Nitrate adsorption was treated as the reply, or outcome variable. The layout of experiments In addition outcomes from every 15 trials, consisting three central points, for zeolite and  $\text{Ca}(\text{OH})_2$  nanoparticles are shown in Tables 1 and 2, respectively. Each experiment was conducted three times to ensure consistency. The collected findings were used to compute the equation's ten coefficients, which show how the independent variables— The adsorption, thermal degree, and pH—and response functions relate to one another. value. Typically in the surface response method a second-order polynomial equation is applied and expressed as follows:

$$Y=b_0+ b_1x_1+ b_2x_2+ b_3x_3+b_{12}x_1x_2+b_{13}x_1x_3+b_{23}x_2x_3+ b_{11}x_1^2+ b_{22}x_2^2+ b_{33}x_3^2 \quad (2)$$

In the proposed model, Y represents the response variable, specifically the percentage of nitrate adsorbed. The independent variables are denoted as follows:  $x_1$  corresponds to pH,  $x_2$  represents thermal degree, and  $x_3$  stands for the quantity of absorbent. The squared variables

are denoted as  $x_{12}$ ,  $x_{22}$ , and  $x_{32}$ , while the interaction element are represented by  $x_{1x2}$ ,  $x_{1x3}$ , and  $x_{2x3}$ .

The linear coefficients are designated as  $b_1$ ,  $b_2$ , and  $b_3$ , while the quadratic coefficients are denoted as  $b_{11}$ ,  $b_{22}$ , and  $b_{33}$ . The interaction coefficients between independent variables are represented by  $b_{12}$ ,  $b_{13}$ , and  $b_{23}$ . Additionally,  $b_0$  represents the model constant.

To assess the interaction between the variables and the responses, On the basis of the suggested model, an Analysis of Variance (ANOVA) was carried out.

**Table 1.** Tabular Data: Zeolite Box-Behnken Design Matrix for Three Parameters; Three Levels Combined With Detected And Projected Values

Exp.Run	X1	X2	X3	reduction%	expected
1	7	45	0.5	29.33	31.61
2	7	35	1.25	31.28	32.48
3	7	25	2	41.90	39.63
4	5	25	1.25	42.71	44.67
5	7	25	0.5	37.65	34.86
6	9	25	1.25	31.89	35.01
7	5	35	2	58.04	58.96
8	5	35	0.5	35.48	36.32
9	9	45	1.25	41.12	39.17
10	9	35	0.5	35.92	35.61
11	7	45	2	49.91	52.71
12	7	35	1.25	33.98	32.47
13	7	35	1.25	32.17	32.46
14	5	45	1.25	53.46	50.35
15	9	35	2	39.66	38.82

<sup>a</sup>The independent variables  $x_1$  (pH),  $x_2$  (temperature), and  $x_3$  (amount of adsorbent) are all related.

**Table 2.** Box-Behnken Design Matrix of  $\text{Ca}(\text{OH})_2$  for Three Variables; Three Levels Together With Observed And Predicted Values

Exp.Run	$X_1$	$X_2$	$X_3$	Removal, %	Predicted
1	7	35	1.25	48.01	49.17
2	5	35	2	60.34	61.42
3	9	25	1.25	40.63	41.52
4	9	35	2	40.20	45.91
5	7	45	0.5	43.77	44.37
6	5	35	0.5	48.52	48.82
7	7	25	0.5	39.65	39.84
8	7	35	1.25	49.37	49.17
9	7	45	2	54.01	53.83
10	5	25	1.25	56.12	55.64
11	7	35	1.25	50.11	49.17
12	5	45	1.25	59.30	58.41
13	9	35	0.5	41.53	40.45
14	7	25	2	49.02	48.43
15	9	45	1.25	48.17	48.65

<sup>a</sup>The independent variables  $x_1$  (pH),  $x_2$  (temperature), and  $x_3$  (amount of adsorbent) are all related.

### 3. Results and discussion

#### 3.1. Characterization of Zeolite and Ca(OH)<sub>2</sub> Nano-particles

Fig. 1 depicts SEM images of micro-particles of zeolite (Fig. 1a) and Ca(OH)<sub>2</sub> (Fig. 1c) before modification, as well as images of nano-particles of zeolite (Fig. 1b) and Ca(OH)<sub>2</sub> (Fig. 1d) after modification. These images show that most of the nanoparticles have a size smaller than 100 nm. The SEM images of zeolite and Ca(OH)<sub>2</sub> in Fig. 1 reveal several changes in surface morphology of the samples after modification. The high shear force applied by the planetary mill resulted in smaller particle sizes. Additionally, the shape of the particles changed from irregular to spherical [56, 57].

The TEM images (Fig. 2) show that the shapes of zeolite and Ca(OH)<sub>2</sub> nanoparticles are spherical, and the diameter of nano-particles is about 1 to 100 nm. Since the nanoparticles are crystalline ones, they are symmetrical circles in shape [55].

Based on Fig. 3 (a), the results of X-ray analysis for zeolite nano-particles show that the largest component of the zeolite is clinoptilolite. Calcite and quartz are other sample ingredients, and they match clinoptilolite-Ca (Ca<sub>3</sub>.16Si<sub>136</sub>O<sub>72</sub>(H<sub>2</sub>O)<sub>21.80</sub>) based on the X-ray curve formula in X'pert Highscore software [22].

Fig. 3 (b) shows the X-ray analysis results of Ca(OH)<sub>2</sub> nano-particles done by X'pert Highscore software and indicates the high purity of Ca(OH)<sub>2</sub> (about 90%). Moreover, the peaks observed at 18.0, 28.3, 30.0, and 54.2 indicate the presence of limes and peaks of 47.0 and 54.7 show the presence of quartz in solid [46].

FTIR testing is a useful method for obtaining sufficient information about the structure and determining the type of functional group and the bonds in its molecules [35]. FTIR spectrum for zeolite is shown in Fig. 4 (a). The nano-particles have peaks at wavelengths between 450 cm<sup>-1</sup> and 3950 cm<sup>-1</sup>. A band at 3627 cm<sup>-1</sup> represents the O-H stretch band [6]. A band at 1641 cm<sup>-1</sup> shows the bending tensile band of water. The bands at 466 cm<sup>-1</sup> and 796 cm<sup>-1</sup> represent Si-O and Al-O, or the Si-O-Si stretching structure, depending on the degree of crystalline phase observed in the material [6, 33]. In addition, a strong vibrational peak at 1048 cm<sup>-1</sup> represents

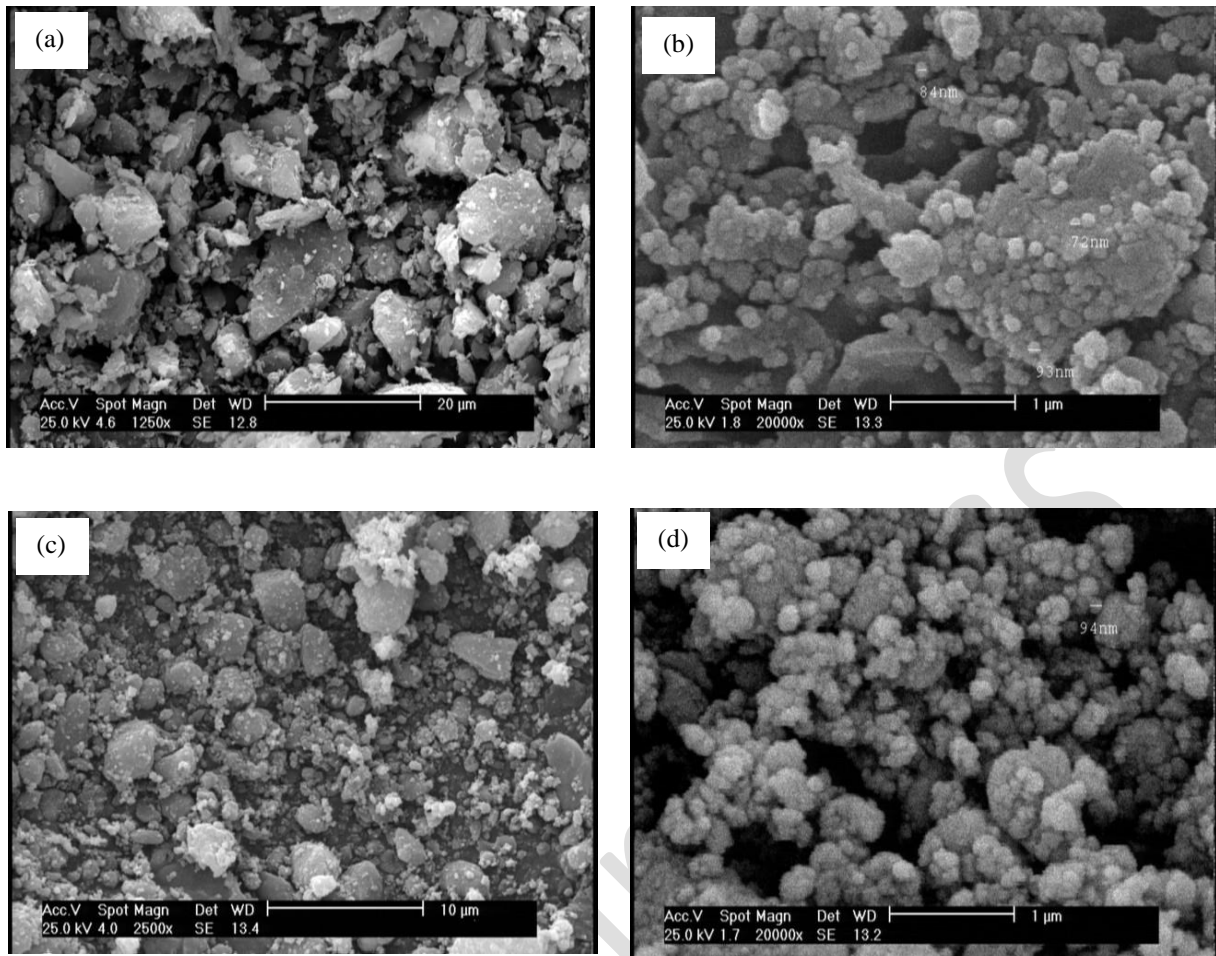


**Fig. 1.** SEM images (a) micro particles of zeolite (b) nano-particle of zeolite (c) micro particles of  $\text{Ca}(\text{OH})_2$  and (d) nano- particles of  $\text{Ca}(\text{OH})_2$ .

the Si-O-Al tensile strain, and the position of this bond depends on Al/Si. The FTIR sample corresponds to the samples taken from the articles [58]. The FTIR spectrum of  $\text{Ca}(\text{OH})_2$  is shown in Fig. 4(b). The narrow absorption band at  $3644\text{ cm}^{-1}$  is due to stretching mode of O-H present in the sample. The absorption bands at  $1463\text{ cm}^{-1}$ ,  $1004\text{ cm}^{-1}$  and  $877\text{ cm}^{-1}$  are assigned to different vibration modes C-O of carbonate groups.

Statistical analysis of data and the statistical significance of independent variables were investigated using ANOVA and Minitab 17 was used to calculate the statistical factors and variables of second-order polynomials. In addition, the quadratic model is a favorable one for predicting the adsorption efficiency of nitrate, and the importance of each coefficient was determined by the values of T and P, as presented in Tables 1 and 2. Multiple regression analysis of experimental data with a confidence level of 95% for zeolite and  $\text{Ca}(\text{OH})_2$  was carried out [59, 60].



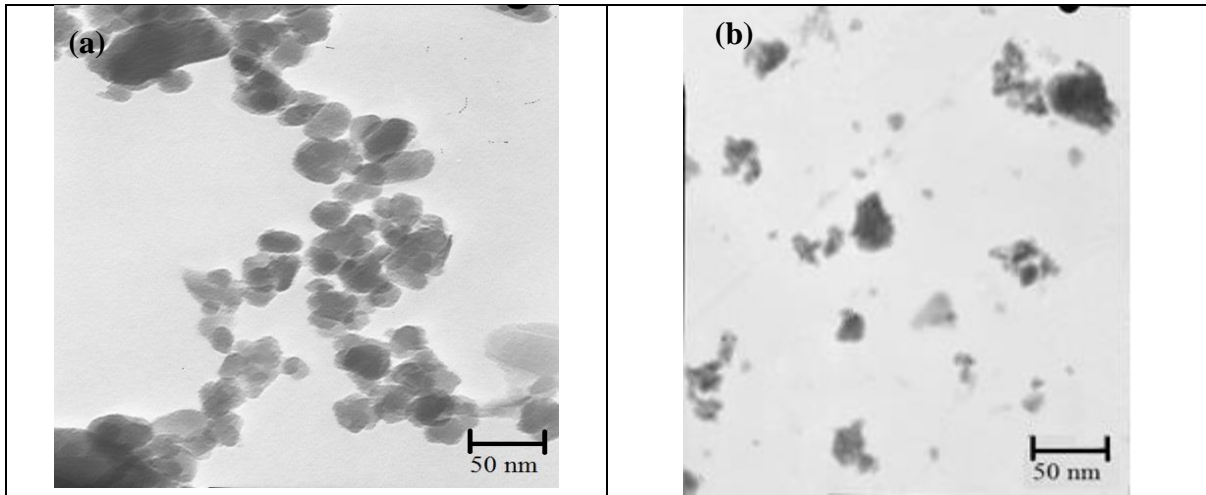


Fig. 2. TEM images nano-particles (a) zeolite (b)  $\text{Ca(OH)}_2$

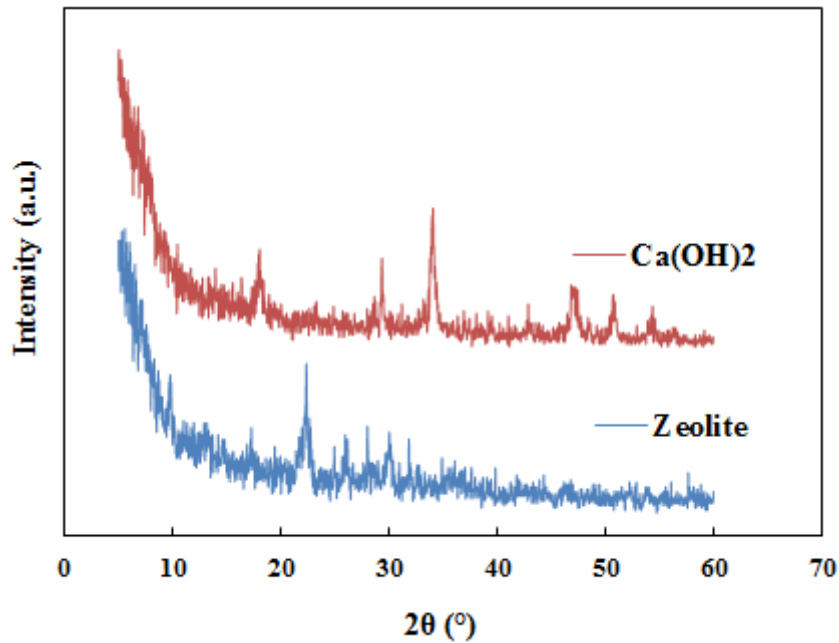


Fig. 3. The XRD pattern of Zeolite and  $\text{Ca(OH)}_2$  nanoparticles

For zeolite nanoparticle in BBD:

$$Y = 32.48 - 5.21X_1 + 2.46 X_2 + 6.47 X_3 + 6.27 X_1 \times X_1 + 3.55 X_2 \times X_2 + 3.68 X_3 \times X_3 - 0.38 X_1 \times X_2 - 4.86 X_1 \times X_3 + 4.08 X_2 \times X_3 \quad (3)$$

Where Y is the removal percentage of nitrate by zeolite nanoparticles. In addition, as already stated,  $x_1$ ,  $x_2$ , and  $x_3$  correspond to pH values, thermal condition, including adsorbent's quantity, respectively. In relation to the significance levels (P-values) presented in chart, the

variables with the greatest impact on nitrate adsorption by zeolite nanoparticles were pH (P=0.008) and quantity of sorbent (P=0.003), Whereas thermal condition (P=0.098) had the least significant impact on nitrate adsorption effectiveness by zeolite nanoparticles.

**Table 3.** Analysis of Variance for the Response Surface Reduced Quadratic Model for zeolite nano-particles

Term	Coefficient	SE Coefficient	T-Value	P-Value
<b>Constant</b>	32.48	1.97	16.45	0.000
<b>X<sub>1</sub></b>	-5.21	1.21	-4.31	0.008
<b>X<sub>2</sub></b>	2.46	1.21	2.03	0.098
<b>X<sub>3</sub></b>	2.47	1.21	5.35	0.003
<b>X<sub>1</sub>X<sub>1</sub></b>	6.27	1.78	3.53	0.017
<b>X<sub>2</sub>X<sub>2</sub></b>	3.55	1.78	1.99	0.103
<b>X<sub>3</sub>X<sub>3</sub></b>	3.68	1.78	2.07	0.094
<b>X<sub>1</sub>X<sub>2</sub></b>	-0.38	1.71	-0.22	0.833
<b>X<sub>1</sub>X<sub>3</sub></b>	-4.86	1.71	-2.84	0.036
<b>X<sub>2</sub>X<sub>3</sub></b>	4.08	1.71	2.39	0.063

The variables aX1, X2, and X3 represent the temperature, pH, and adsorbent quantity.

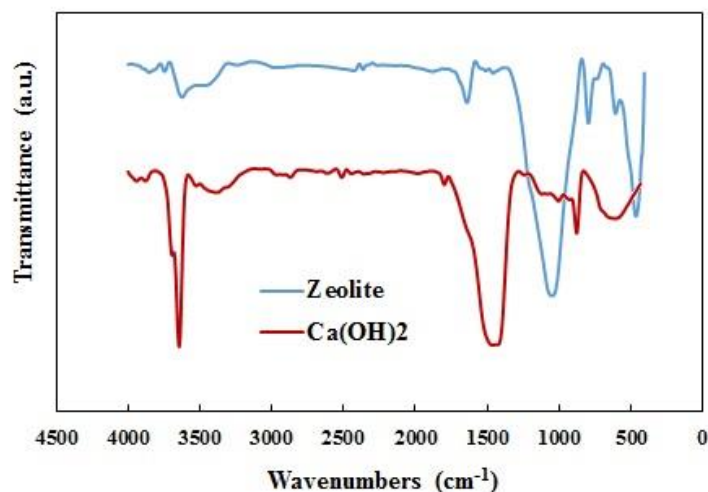


**Fig. 4.** The Fourier transform infrared spectra of zeolite and Ca(OH)<sub>2</sub> nanoparticles.

Based on the ANOVA results, the interaction of the parameters was found significant when  $P < 0.05$  except for the thermal condition ( $P=0.098$ ); the synergistic thermal degree and pH effects was observed when  $P=0.833$ ; the combined temperature's impact and quantity of sorbent was also noteworthy when  $P=0.063$ . The ultimate predicted mathematical model in terms of the

importance of the actual variables for nitrate adsorption (Y) by the zeolite nanoparticles is outlined below:

$$Y=32.48 - 5.21 X_1+ 6.47 X_3 + 6.27 X_1 \times X_1 - 4.86 X_1 \times X_3 \quad (4)$$

The regression coefficient associated with this model (R=0.934) shows that only 5.7% of the changes are not foreseeable according to the model. The highest level of adsorption rate of nitrate was 58.04%.

Table 4 shows the analysis of variance of zeolite nano particles. Results show that the P-Value=0.095 and it is greater than 0.05, indicating suitable model and fit. In addition, we do not have enough evidence to express the existence of lack of fit.

**Table 4.** Analysis of variance of Zeolite nano particles

Source	DF	Adj SS	Adj MS	F-Value	P-Value
<b>Model</b>	9	952.01	105.779	8.98	0.013
<b>Linear</b>	3	586.30	195.433	16.58	0.005
<b>pH</b>	1	211.15	211.151	17.92	0.008
<b>T</b>	1	48.36	48.364	4.10	0.099
<b>Gr</b>	1	326.78	326.785	27.73	0.003
<b>Square</b>	3	209.92	69.974	5.94	0.042
<b>pH*pH</b>	1	141.84	141.837	12.04	0.018
<b>T*T</b>	1	48.40	48.397	4.11	0.099
<b>Gr*Gr</b>	1	47.86	47.863	4.06	0.100
<b>2-Way Interaction</b>	3	155.79	51.931	4.41	0.072
<b>pH*T</b>	1	0.58	0.578	0.05	0.834
<b>pH*Gr</b>	1	88.55	88.548	7.51	0.041
<b>T*Gr</b>	1	66.67	66.667	5.66	0.063
<b>Error</b>	5	58.92	11.785		
<b>Lack-of-Fit</b>	3	55.14	18.379	9.71	0.095
<b>Pure Error</b>	2	3.79	1.893		
<b>Total</b>	14	1010.94			

For Ca(OH)<sub>2</sub> nano-particles, Table 5 shows the following equation:

$$Y= 49.163 - 5.969 X_1 + 2.479 X_2 + 4.512 X_3 + 2.213 X_1 \times X_1 - 0.322 X_2 \times X_2 - 2.229 X_3 \times X_3 + 1.090 X_1 \times X_2 - 1.787 X_1 \times X_3 + 0.217 X_2 \times X_3 \quad (5)$$

The variables with the highest effect on nitrate adsorption by Ca(OH)<sub>2</sub> nano-particles include  
 The final anticipated mathematical model for nitrate adsorption (Y) by Ca(OH)<sub>2</sub> nanomaterials is generally provided below, taking into account the importance of real variables:

Temperature (P=0.002), pH (P=0.000), and adsorbent quantity (P=0.000). It was determined that the pH and adsorbent quantity impact of interaction (P=0.034) was appropriate.

$$Y = 49.163 - 5.969 X_1 + 2.479 X_2 + 4.512 X_3 + 2.213 X_1 \times X_1 - 2.229 X_3 \times X_3 - 1.787 X_1 \times X_3 \quad (6)$$

The regression coefficient for this model (R=0.986) shows that only 1.4% of the changes are not predictable by the model. The maximum adsorption rate of nitrate by Ca(OH)<sub>2</sub> nanoparticles was determined as 60.34%.

**Table 5.** Analysis of Variance for the Response Surface Reduced Quadratic Model for Ca(OH)<sub>2</sub> nanoparticles

Term	Coefficient	SE Coefficient	T-Value	P-Value
<b>Constant</b>	49.17	0.71	69.17	0.000
<b>X<sub>1</sub></b>	-5.97	0.44	-13.71	0.000
<b>X<sub>2</sub></b>	2.48	0.44	5.70	0.002
<b>X<sub>3</sub></b>	4.51	0.44	10.37	0.000
<b>X<sub>1</sub>X<sub>1</sub></b>	2.21	0.64	3.45	0.018
<b>X<sub>2</sub>X<sub>2</sub></b>	-0.32	0.64	-0.50	0.637
<b>X<sub>3</sub>X<sub>3</sub></b>	-2.23	0.64	-3.45	0.018
<b>X<sub>1</sub>X<sub>2</sub></b>	1.09	0.62	1.77	0.137
<b>X<sub>1</sub>X<sub>3</sub></b>	-1.79	0.62	2.90	0.034
<b>X<sub>2</sub>X<sub>3</sub></b>	0.22	0.62	0.35	0.738
aX <sub>1</sub> , X <sub>2</sub> , and X <sub>3</sub> represent the temperature, adsorbent quantity, and pH.				

Analysis of variance of Ca(OH)<sub>2</sub> nano particles are shown in Table 6. The results show that P-Value=0.150 and it is greater than 0.05, which implies that in this case suitable model and fit was selected and not enough evidence to express the existence of lack of fit.

**Table 6.** Analysis of variance of Ca(OH)<sub>2</sub> nano particles

Source	DF	Adj SS	Adj MS	F-Value	P-Value
<b>Model</b>	9	615.483	68.387	28.53	0.001
<b>Linear</b>	3	523.538	174.513	72.80	0.000
<b>pH</b>	1	361.133	361.133	150.64	0.000
<b>T</b>	1	49.154	49.154	20.50	0.006
<b>Gr</b>	1	113.251	113.251	47.24	0.001
<b>Square</b>	3	43.773	14.591	6.09	0.040
<b>pH*pH</b>	1	9.295	9.295	3.88	0.106
<b>T*T</b>	1	1.124	1.124	0.47	0.524
<b>Gr*Gr</b>	1	30.114	30.114	12.56	0.016
<b>2-Way Interaction</b>	3	48.172	16.057	6.70	0.033
<b>pH*T</b>	1	4.752	4.752	1.98	0.218
<b>pH*Gr</b>	1	43.231	43.231	18.03	0.008
<b>T*Gr</b>	1	0.189	0.189	0.08	0.790
<b>Error</b>	5	11.986	2.397		
<b>Lack-of-Fit</b>	3	10.753	3.584	5.81	0.150
<b>Pure Error</b>	2	1.233	0.617		
<b>Total</b>	14	627.470			

### 3.3. Effect of Parameters on Nitrate adsorption

The contour charts represent independent parameters with the identical answer value, Y. The contour plots for every parameter and factor show the relationship between the first and third parameters while keeping a constant parameter. In all experiments conducted in this study, two parameters were variable while one parameter was kept constant. The most effective parameters in the adsorption of nitrate by zeolite and Ca(OH)<sub>2</sub> nanoparticles were found to be pH, temperature, and the quantity of adsorbent. According to the Box-Benken Design (BBD), the optimal settings of independent variables for zeolite and Ca(OH)<sub>2</sub> nanoparticles were 5 for pH, 45°C for temperature, and 2 g for the amount of adsorbent.

#### 3.3.1. The Impact of pH

The pH is an important parameter that affects the absorption process [14]. To investigate the effect of pH on the absorption capacity of zeolite and Ca(OH)<sub>2</sub> nanoparticles for nitrate adsorption, experiments were conducted with variable pH values ranging from 5 to 9. The

optimal pH value obtained based on the response of the Box-Behnken Design was found to be 5. The effect of pH on temperature and the amount of adsorbent for zeolite nanoparticles is shown in Figs. 5A and B, while similar curves for  $\text{Ca}(\text{OH})_2$  nanoparticles are shown in Fig. 6A and B.

As illustrated, the percentage of nitrate adsorption decreased as the pH raised from 5 to 9, with the same adsorbent concentration temperatures. The peak percentage of nitrate adsorption occurred in an acidic environment due to the adsorption of nitrate by zeolite and  $\text{Ca}(\text{OH})_2$  nanoparticles. According to studies conducted in an acidic pH environment, the concentration of  $\text{H}^+$  ions is high in the solution. Additionally, this action generates a positive charge on the surface of the adsorbents, which enhances adsorbent surface absorption in the acidic pH environment of nitrate, which has a negative charge. At higher pH levels in an alkaline environment, the concentration of  $\text{OH}^-$  ions is high, creating a negative charge on the surface of the adsorbents. The presence of zeolite nanoparticles contributes to this effect, as the interaction between the hydroxyl group and silicon ( $\text{Si-OH}$ ) in the minerals decreases the active sites of adsorption at a mineral level. As a result, the mineral absorption capacity is reduced, resulting in the elimination of nitrate pollutant adsorption from the adsorbent surface [4, 61].

### **3.3.2. The Effect of Temperature**

The effect of temperature on nitrate absorption by zeolite and  $\text{Ca}(\text{OH})_2$  nanoparticles was investigated in the temperature range of 25 to 45 ° C. Fig. 5 C and B for zeolite nanoparticles and Fig. 6 C and B for  $\text{Ca}(\text{OH})_2$  nanoparticles demonstrate the combined influence of temperature, pH, and amount of sorbent. Based on the outcome, the adsorption percentage increases as temperature increases and the energy of ion molecular movement increases in the solution, which, in turn, increases the probability of contact with the active sites of the surface.

### **3.3.3. The effect of adsorbents dosage**

Another important parameter in the adsorption process is the amount of adsorbent used in the process [61-63]. The findings show that when the quantity of sorbent increases from 0.5 to 2 grams with a constant pH and thermal degree, as shown in Fig.5 B and C for zeolite nanoparticles and in Fig. 6 B and C for  $\text{Ca}(\text{OH})_2$  nanoparticles, the amount of nitrate adsorption increases, too. The analysis of the surface of the Box-Behnken showed that the optimal quantity of sorbent for nitrate adsorption was 2 grams. The adsorption rates may increase by increasing the quantity of sorbent ranging from 0.5 grams to 2 grams, thus leading to an increase in the

number of adsorption sites, adsorbent, and adsorption material groups, and absorption capacity. Therefore, access to active sites is more convenient at absorbent levels [62, 64, 65].

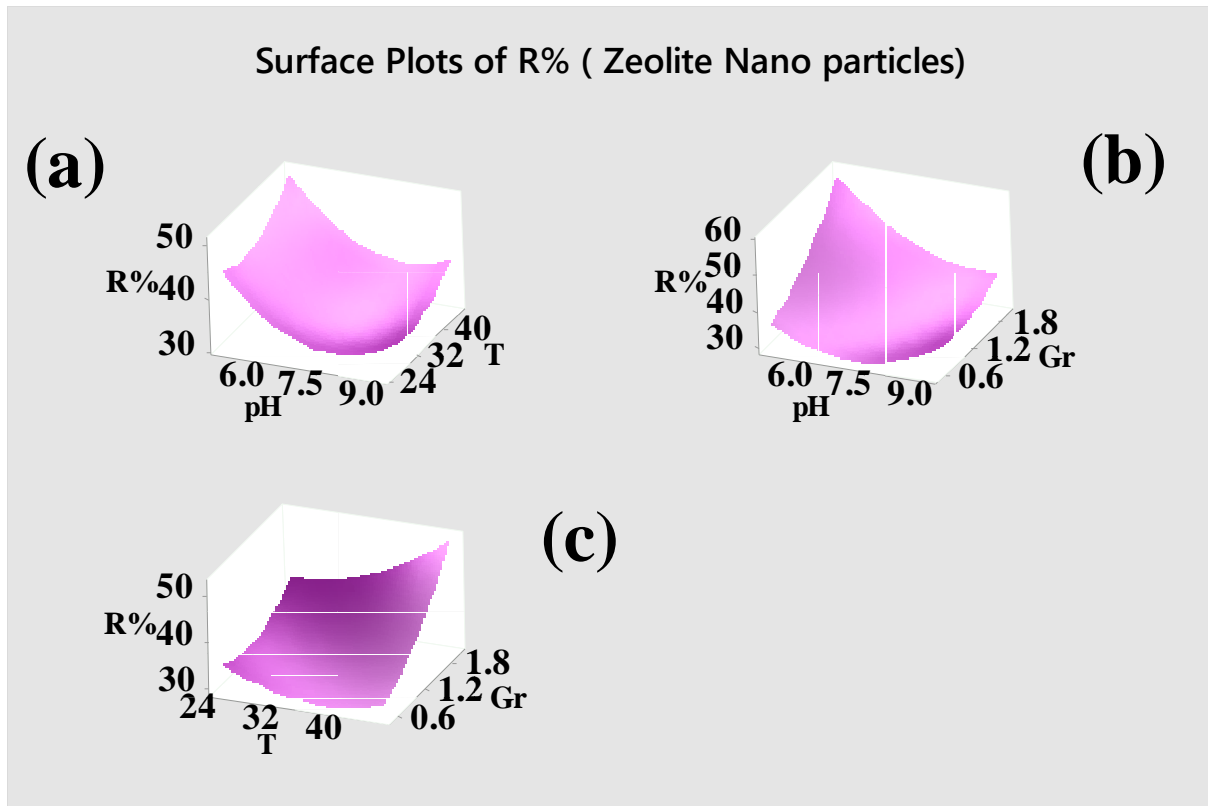


**Fig. 5.** Zeolite nanoparticle's three-dimensional response surface plot for zeolite nanoparticles: a) mixed impact of  $x_1$  and  $x_2$ , b) combined effect of  $x_1$  and  $x_3$ , and c) combined effect of  $x_2$  and  $x_3$ .

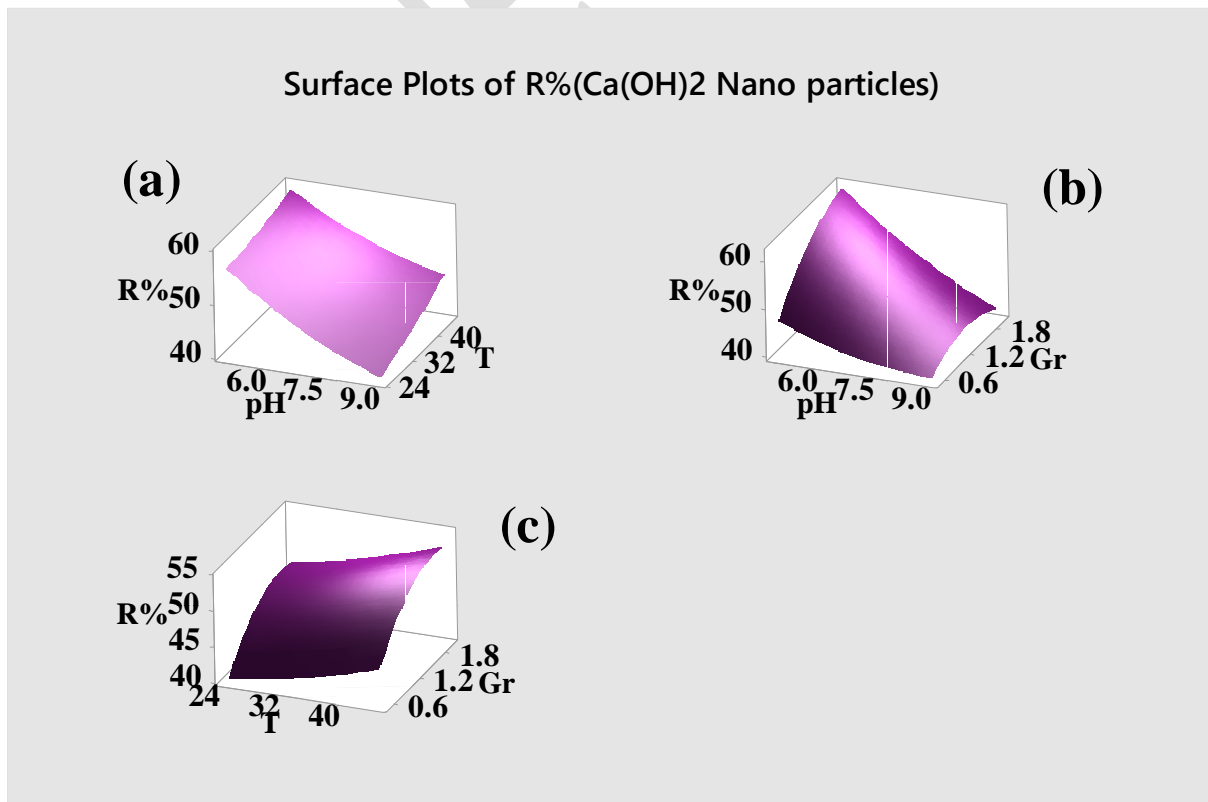


**Fig. 6:** Ca(OH)<sub>2</sub> nanoparticle's three-dimensional response surface plot For Ca(OH)<sub>2</sub> nanoparticle, the combined effects of x<sub>1</sub> and x<sub>2</sub>, x<sub>1</sub> and x<sub>3</sub>, and x<sub>2</sub> and x<sub>3</sub> are shown in a) the combined effect and b) the combined effect.

### **3.4. Comparing the results of adsorption for nitrate removal using natural Ca(OH)<sub>2</sub> and zeolite**

#### **3.4.1 Adsorbent usage**

Natural Ca(OH)<sub>2</sub> and zeolite typically require lower dosages compared to other adsorbents such as ion exchange resins or activated charcoal to remove nitrates.

The usage of Natural Ca(OH)<sub>2</sub> and zeolite may result in cost savings due to their lower dosage requirements.

#### **3.4.1 Removal Performance**

Zeolite generally exhibits higher nitrate removal efficiency compared to activated carbon, ion exchange resins, or other adsorbents due to its specific structure and surface properties.

Natural Ca(OH)<sub>2</sub> also shows good nitrate removal performance, but may be less effective than zeolite in some cases.

#### **3.4.2 pH**

The pH of the solution can significantly impact the adsorption capacity of different adsorbents. For example, ion exchange resins may have specific pH requirements for optimal performance. Natural Ca(OH)<sub>2</sub> and zeolite are generally effective over a wide range of pH values, making them versatile options for nitrate removal.

#### **3.4.3 Temperature**

Temperature can influence the kinetics and equilibrium of adsorption processes. Some adsorbents may exhibit better performance at higher temperatures.

Natural Ca(OH)<sub>2</sub> and zeolite are known to be effective at a wide range of temperatures, making them suitable for various applications.

#### **3.4.4 Time Duration**



The contact time required for effective nitrate removal can vary depending on the adsorbent used. Some adsorbents may require longer contact times to achieve desired removal efficiencies.

Natural Ca(OH)<sub>2</sub> and zeolite typically exhibit relatively fast adsorption kinetics, allowing for efficient nitrate removal within a reasonable time duration.

In conclusion, Natural Ca(OH)<sub>2</sub> and zeolite offer advantages in terms of adsorbent usage, removal performance, pH tolerance, temperature sensitivity, and time duration compared to other available adsorbents used in the past for nitrate removal. Their versatility, cost-effectiveness, and efficiency make them attractive options for various water treatment applications.

### 3.5. Kinetic Studies

Adsorption kinetics show changes in adsorbent concentrations with time variations that are defined as absorption rates [41, 66]. Kinetic parameters play a crucial part in predicting the amount of absorption and providing important information for modelling it. In this study, the absorption kinetic data were obtained from pseudo-first-order and pseudo-second-order models and these kinetic models are widely used [67-69]. The effect of contact time on adsorption of zeolite and Ca(OH)<sub>2</sub> nanoparticles in (pH level of 5, temperature of 45 degrees Celsius, and amount of adsorbent at 2 grams) was investigated. The pseudo-first-order and pseudo-second-order kinetic models and their parameters are shown in Table 7 [70]:

**Table 7.** The pseudo-first-order and pseudo-second-order kinetic models and their parameters

Kinetic model	Equation	Parameters
<b>pseudo-first-order</b>	$1qt=k1(qet)+ 1qe$	$q_e$ : the adsorption capacity in equilibrium (mg), $q_t$ : the amount of nitrate adsorbed by nanoparticles in equilibrium (mg), $k_1$ : the constant pseudo-first-order rate of adsorption (1/min).
<b>pseudo-second-order</b>	$tqt=1qet+[ 1K2$ $qe2]$	$K_2$ : the pseudo-second-order rate constant parameter of adsorption (g/mg/min).

The values of  $q_e$  and  $q_t$  are obtained through the following equations:

$$qt=C0 - Ce \times VW \tag{7}$$

Where  $C_0$  and  $C_e$  represent the initial and final concentrations of nitrate in a solution, respectively.  $V(L)$  denotes the volume of the solution, while  $m(g)$  indicates the quantity of adsorbent mass utilized.

The comparison between adsorption kinetic models shows that the second-order pseudo kinetic model is highly compatible with experimental data for both nano-particles. The pseudo-second-order kinetic plot is obtained in  $t/q_t$  according to  $t$  in an integrated straight line.  $R_{zeolite} = 0.9910$  (Fig.7) and  $R_{Ca(OH)_2} = 0.9984$  (Fig.8). Based on the results obtained, the amount of nitrate removed by  $Ca(OH)_2$  and zeolite nano-particles in the first 15 minutes was 51.62% and 48.46%, respectively. The two-step process of nitrate adsorption is fast and proceeds at a faster rate, because, at the beginning of the reaction, the number of occupational groups and adsorption sites is higher at the level of adsorption. Gradually, these places were occupied and reduced in number; however, over time, significant changes that took 90 minutes to appear in the percentage adsorption by both nano-particles were not observed [67, 69, 71].

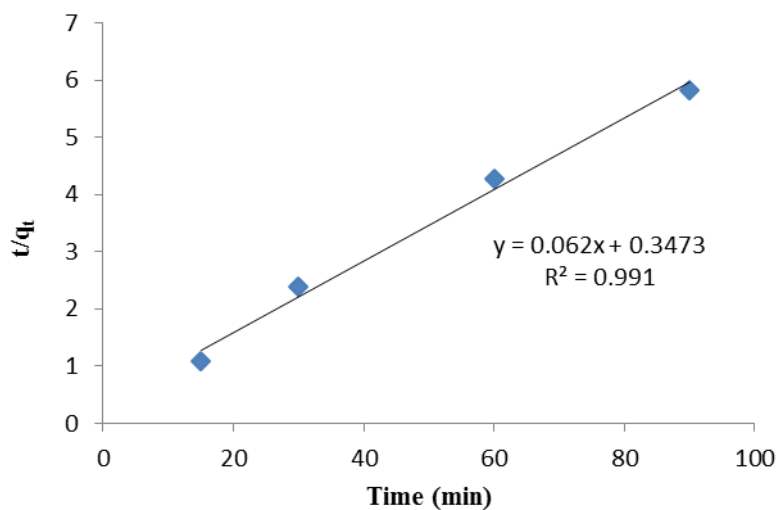


**Fig. 7.** Pseudo-second order kinetic plot for the adsorption of nitrate Zeolite nano-particles amount of adsorbent = 2 g; temperature= 45°C and pH =5

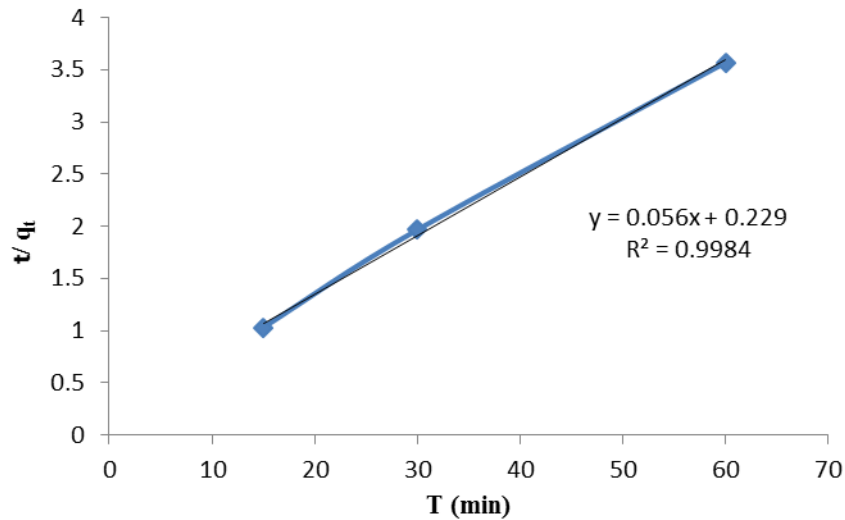


**Fig. 8.** Pseudo-second order kinetic plot for the adsorption of nitrate  $\text{Ca}(\text{OH})_2$  nano-particles amount of adsorbent = 2 g; temperature=  $45^\circ\text{C}$  and  $\text{pH} = 5$

### 3.6. Adsorption Isotherms

The correlation between nitrate Content and the amount of nitrate Absorbed by  $\text{Ca}(\text{OH})_2$  and zeolite nanoparticles with Langmuir and Freundlich models were investigated. In Langmuir isotherm, all adsorption sites are found on the absorbing surface, and each absorption region can absorb only one species on its surface [70, 72-75]. The Langmuir and Freundlich isotherm equations are presented in Table 8.

**Table 8.** The Langmuir and Freundlich models and their parameters

Isotherm model	Equation	Parameters
<b>Langmuir</b>	$ceq = \frac{1}{\frac{1}{K_L q_{max}} + \frac{1}{C_e}}$	The equilibrium capacity of nitrate on the adsorbents at equilibrium time is expressed as $q_e$ (mg/g). $C_e$ (mg/L) is the nitrate equilibrium concentration; $q_{max}$ (mg/g) is the adsorbents' maximum capacity. The Langmuir constant is $K_L$ (L/mg), which is defined as the energy of absorption correlation.
<b>Freundlich</b>	$\text{Log } q_e = \text{Log } K_F + \frac{1}{n} \text{Log } C_e$	$K_F$ (mg/g): the Freundlich constant $1/n$ : the intensity factor of surface absorption, which varies between 0 and 1.

The constant and meaningless variable in isotherm, which represents the isotherm type, is defined as  $R_L$ , as shown in the following formula:

$$R_L = 1 + K_L C_e \quad (8)$$

Where  $K_L$  and The equilibrium concentration ( $C_e$ ) shares a similar concept with the Langmuir equation, In addition, the values indicate that if the value of  $R_L$  ranges between 0 and 1, desired absorption is observed; if that of  $R_L$  is greater than 1, undesirable absorption is anticipated. If  $R_L$  is equal to 1, linear absorption is expected; if  $R_L$  is equal to zero, irreversible absorption is anticipated [76, 77]. Fig. 9 shows the Langmuir isotherm model for zeolite nanoparticle, and Fig. 10 represents the Langmuir model for  $\text{Ca}(\text{OH})_2$ . At isotherm Freundlich, absorption occurs on a heterogeneous surface [75].

To investigate the nitrate uptake capacity of  $\text{Ca}(\text{OH})_2$  and zeolite nanoparticles, the concentration of nitrate at 25, 50, 100, and 150 mg/l was studied in equilibrium conditions. The Freundlich and Langmuir isotherms' correlation coefficients were determined at a pH of 5, with an adsorbent amount of 2 g, a temperature of 45°C, and a duration of 45 minutes. For  $\text{Ca}(\text{OH})_2$  and zeolite nano-particles were 0.9695 & 0.8343 and 0.9938 & 0.9993, respectively. As indicated, the Langmuir isotherm absorbs nitrate better on both nanoparticles, as explained earlier. The value of  $R_L$  for  $\text{Ca}(\text{OH})_2$  and zeolite nanoparticles is measured as 0.714 and 0.769, respectively, representing excellent absorption for both  $\text{Ca}(\text{OH})_2$  and zeolite nano-particles. A previous study concerning the adsorption of nitrate by Chitosan/Zeolite Y/Nano  $\text{ZrO}_2$  nanocomposite and polyacrylonitrile–alumina nano-particle showed that the adsorption of the nitrate model was of Langmuir [48].

### 3.6.1 The adsorption isotherms in the dynamic model

In the context of adsorption isotherms in the dynamic mode, it is important to understand that adsorption isotherms describe the relationship between the amount of adsorbate (substance being adsorbed) on the surface of an adsorbent material at equilibrium and the concentration of the adsorbate in the bulk phase. In dynamic mode, the adsorbate is continuously flowing over the adsorbent material, allowing for a dynamic equilibrium to be established between the adsorbate in the bulk phase and the adsorbate on the surface of the adsorbent.

One commonly used model to describe adsorption in dynamic mode is the Langmuir model, which assumes a monolayer adsorption process with a finite number of identical sites on the adsorbent surface. The Langmuir equation can be expressed as:

$$q/C = q_{\max} K_L / (1 + K_L C) \quad (9)$$

where:

$q$  is the amount of adsorbate adsorbed per unit mass of adsorbent at equilibrium,

$C$  is the concentration of the adsorbate in the bulk phase,

$q_{\max}$  is the maximum adsorption capacity of the adsorbent,

$K_L$  is the Langmuir constant related to the affinity of the adsorbate-adsorbent interaction.

Desorption efficiency refers to the ability of an adsorbent material to release or desorb the previously adsorbed molecules under certain conditions. The desorption efficiency can be influenced by factors such as temperature, pressure, and the nature of the adsorbate-adsorbent interaction.

For example, at a specific temperature, one can study the desorption efficiency of an adsorbent by measuring the amount of adsorbate desorbed from the adsorbent material under controlled conditions. This can be expressed as a percentage of the initial amount of adsorbate adsorbed. The desorption efficiency can be calculated using the formula:

$$\text{Desorption Efficiency (\%)} = \frac{\text{Amount of Adsorbate Desorbed}}{\text{Initial Amount of Adsorbate Adsorbed}} \times 100\%$$

By studying desorption efficiency at different temperatures, one can gain insights into the desorption behavior of the adsorbent material and optimize conditions for efficient desorption processes in dynamic adsorption systems.

### **3.7. Investigation of the mixture of $\text{Ca}(\text{OH})_2$ and zeolite nanoparticles in nitrate adsorption**

Here, the optimal values of temperature, adsorption, and contact time parameters for lime and zeolite minerals were considered the same. To test the application of a mixture of two adsorbents, three experiments were carried out with different ratios of nanoparticles. The conditions for each experiment and the values obtained for elimination are given in Table 9.

**Table 9.** Nitrate adsorption experiments with Ca(OH)<sub>2</sub> and zeolite mixtures

No	pH	Temperature (°C)	Amount of adsorbent	Removal%
1	5	45	100% zeolite	53.46%
2	5	45	100% Ca(OH) <sub>2</sub>	59.36%
3	5	45	75% Zeolite+ 25% Ca(OH) <sub>2</sub>	48.98%
4	5	45	50% Zeolite + 50% Ca(OH) <sub>2</sub>	40.81%
5	5	45	25% Zeolite + 75% Ca(OH) <sub>2</sub>	52.13%

The mixture of these nanoparticles together reduced the absorption, while, in the reaction, the amount of Ca(OH)<sub>2</sub> and its reaction with higher zeolite content was observed to be high. These nanoparticles exerted a negative effect on each other.

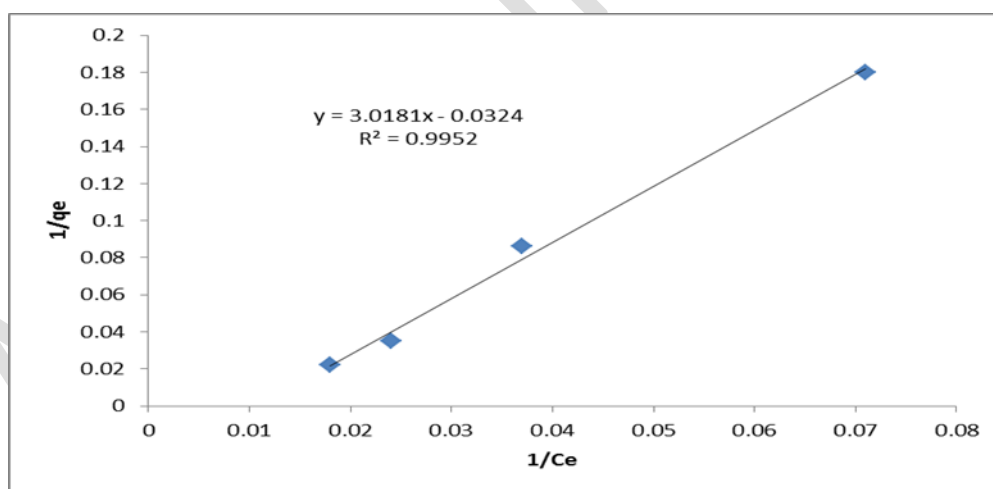


**Fig. 9.** Langmuir isotherm model for nitrate adsorption by nano-particles of Zeolite, volume of adsorbent = 2 g; temperature= 45°C and pH =5

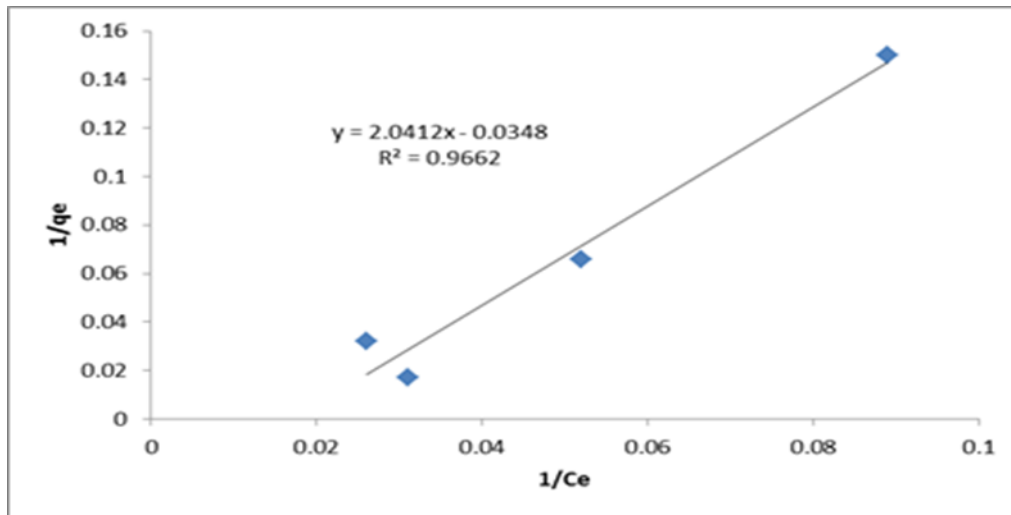


**Fig.10.** Langmuir isotherm model for nitrate adsorption by nano-particles of  $\text{Ca}(\text{OH})_2$  adsorbent weight = 2 g; pH = 5, temperature =  $45^\circ\text{C}$

### 3.7.1. Analyzing adsorbents of $\text{Ca}(\text{OH})_2$ and zeolite

When comparing Natural  $\text{Ca}(\text{OH})_2$  and zeolite as adsorbents for nitrate removal, several aspects need to be considered:

### 3.7.2. Cost

Natural  $\text{Ca}(\text{OH})_2$  is relatively inexpensive compared to zeolite, which is a more specialized and costly adsorbent.

### 3.7.3. Performance

Zeolite has a higher adsorption capacity for nitrate compared to Natural  $\text{Ca}(\text{OH})_2$  due to its specific structure and surface properties.

Natural  $\text{Ca}(\text{OH})_2$  may require more frequent regeneration or replacement due to its lower adsorption capacity.

### 3.7.4. Environmental impact

Both Natural  $\text{Ca}(\text{OH})_2$  and zeolite are considered environmentally friendly adsorbents as they are natural materials.

However, the disposal of spent Natural  $\text{Ca}(\text{OH})_2$  may lead to an increase in calcium ion concentration in water, which could potentially cause hardness issues.

### 3.7.5. Regeneration

Zeolite can readily regenerate via washing with an appropriate solution. While Natural  $\text{Ca(OH)}_2$  may require more complex regeneration processes.

In conclusion, zeolite is a more effective adsorbent for nitrate removal compared to Natural  $\text{Ca(OH)}_2$  in terms of performance and regeneration. However, Natural  $\text{Ca(OH)}_2$  may be a more cost-effective option for applications where high nitrate removal efficiency is not critical. The potential increase in calcium ion concentration in water due to the dissolution of  $\text{Ca(OH)}_2$  should be carefully considered and managed to prevent any adverse effects on water quality.

## 4. Conclusion

In this study,  $\text{Ca(OH)}_2$  and zeolite nanoparticles were studied as low-cost adsorbents for nitrate adsorption in synthetic aqueous solutions. The design of the Box-Behnken test was used to optimize the parameters and the amount of nitrate removed by  $\text{Ca(OH)}_2$  and zeolite nanoparticles. Optimum conditions for the maximum adsorption rate of nitrate by both nanoparticles were characterized as pH 5, temperature of 45 °C, and a total of 2 grams of adsorbent material was used. Kinetic studies revealed that the adsorption of nitrate by nanoparticles followed the pseudo second-order model. Moreover, Langmuir isotherms fit well with isotherm adsorption data. Natural  $\text{Ca(OH)}_2$  and zeolite, characterized by cost-effectiveness and widespread abundance, have the capacity for being used as adsorbents for nitrate adsorption.

## References

1. Tong, Y., & He, Z. (2013). Nitrate removal from groundwater driven by electricity generation and heterotrophic denitrification in a bioelectrochemical system. *Journal of hazardous materials*, 262, 614-619.
2. Öztürk, N., & Bektaş, T. E. (2004). Nitrate removal from aqueous solution by adsorption onto various materials. *Journal of hazardous materials*, 112(1-2), 155-162.
3. Li, J., Li, Y., & Meng, Q. (2010). Removal of nitrate by zero-valent iron and pillared bentonite. *Journal of hazardous materials*, 174(1-3), 188-193.
4. Bhatnagar, A., & Sillanpää, M. (2011). A review of emerging adsorbents for nitrate removal from water. *Chemical engineering journal*, 168(2), 493-504.
5. Palko, J. W., Oyarzun, D. I., Ha, B., Stadermann, M., & Santiago, J. G. (2018). Nitrate removal from water using electrostatic regeneration of functionalized adsorbent. *Chemical Engineering Journal*, 334, 1289-1296.
6. Zavareh, S., Farrokhzad, Z., & Darvishi, F. (2018). Modification of zeolite 4A for use as an adsorbent for glyphosate and as an antibacterial agent for water. *Ecotoxicology and environmental safety*, 155, 1-8.
7. Hosseini, S. M., Ataie-Ashtiani, B., & Kholghi, M. (2011). Nitrate reduction by nano-Fe/Cu particles in packed column. *Desalination*, 276(1-3), 214-221.



8. Shubair, T., Eljamal, O., Khalil, A. M., & Matsunaga, N. (2018). Multilayer system of nanoscale zero valent iron and Nano-Fe/Cu particles for nitrate removal in porous media. *Separation and purification technology*, 193, 242-254.
9. Tyagi, S., Rawtani, D., Khatri, N., & Tharmavaram, M. (2018). Strategies for nitrate removal from aqueous environment using nanotechnology: a review. *Journal of water process engineering*, 21, 84-95.
10. Mukherjee, R., & De, S. (2014). Adsorptive removal of nitrate from aqueous solution by polyacrylonitrile–alumina nanoparticle mixed matrix hollow-fiber membrane. *Journal of membrane science*, 466, 281-292.
11. He, Y., Lin, H., Dong, Y., Li, B., Wang, L., Chu, S., ... & Liu, J. (2018). Zeolite supported Fe/Ni bimetallic nanoparticles for simultaneous removal of nitrate and phosphate: synergistic effect and mechanism. *Chemical Engineering Journal*, 347, 669-681.
12. Bao, Z., Hu, Q., Qi, W., Tang, Y., Wang, W., Wan, P., ... & Yang, X. J. (2017). Nitrate reduction in water by aluminum alloys particles. *Journal of environmental management*, 196, 666-673.
13. Bhatnagar, A., Kumar, E., & Sillanpää, M. (2010). Nitrate removal from water by nano-alumina: Characterization and sorption studies. *Chemical engineering journal*, 163(3), 317-323.
14. Li, P., Lin, K., Fang, Z., & Wang, K. (2017). Enhanced nitrate removal by novel bimetallic Fe/Ni nanoparticles supported on biochar. *Journal of Cleaner Production*, 151, 21-33.
15. Keshvardoostchokami, M., Babaei, S., Piri, F., & Zamani, A. (2017). Nitrate removal from aqueous solutions by ZnO nanoparticles and chitosan-polystyrene–Zn nanocomposite: Kinetic, isotherm, batch and fixed-bed studies. *International journal of biological macromolecules*, 101, 922-930.
16. Li, L., Quinlivan, P. A., & Knappe, D. R. (2002). Effects of activated carbon surface chemistry and pore structure on the adsorption of organic contaminants from aqueous solution. *Carbon*, 40(12), 2085-2100.
17. Quinlivan, P. A., Li, L., & Knappe, D. R. (2005). Effects of activated carbon characteristics on the simultaneous adsorption of aqueous organic micropollutants and natural organic matter. *Water research*, 39(8), 1663-1673.
18. Kul, A. R., & Koyuncu, H. (2010). Adsorption of Pb (II) ions from aqueous solution by native and activated bentonite: kinetic, equilibrium and thermodynamic study. *Journal of Hazardous materials*, 179(1-3), 332-339.
19. Rathnayake, S. I., Xi, Y., Frost, R. L., & Ayoko, G. A. (2016). Environmental applications of inorganic–organic clays for recalcitrant organic pollutants removal: Bisphenol A. *Journal of colloid and interface science*, 470, 183-195.
20. Zhu, R., Zhou, Q., Zhu, J., Xi, Y., & He, H. (2015). Organo-clays as sorbents of hydrophobic organic contaminants: sorptive characteristics and approaches to enhancing sorption capacity. *Clays and Clay Minerals*, 63(3), 199-221.
21. Koubaissy, B., Joly, G., Batonneau-Gener, I., & Magnoux, P. (2011). Adsorptive removal of aromatic compounds present in wastewater by using dealuminated faujasite zeolite. *Industrial & Engineering Chemistry Research*, 50(9), 5705-5713.
22. Wang, S., Li, H., Xie, S., Liu, S., & Xu, L. (2006). Physical and chemical regeneration of zeolitic adsorbents for dye removal in wastewater treatment. *Chemosphere*, 65(1), 82-87.
23. Babel, S., & Kurniawan, T. A. (2003). Low-cost adsorbents for heavy metals uptake from contaminated water: a review. *Journal of hazardous materials*, 97(1-3), 219-243.
24. Caputo, D., & Pepe, F. (2007). Experiments and data processing of ion exchange equilibria involving Italian natural zeolites: a review. *Microporous and Mesoporous Materials*, 105(3), 222-231.

25. Hor, K. Y., Chee, J. M. C., Chong, M. N., Jin, B., Saint, C., Poh, P. E., & Aryal, R. (2016). Evaluation of physicochemical methods in enhancing the adsorption performance of natural zeolite as low-cost adsorbent of methylene blue dye from wastewater. *Journal of cleaner production*, 118, 197-209.
26. Mazloomi, F., & Jalali, M. (2016). Ammonium removal from aqueous solutions by natural Iranian zeolite in the presence of organic acids, cations and anions. *Journal of Environmental Chemical Engineering*, 4(1), 240-249.
27. Crini, G. (2006). Non-conventional low-cost adsorbents for dye removal: a review. *Bioresource technology*, 97(9), 1061-1085.
28. Meng, Q., Chen, H., Lin, J., Lin, Z., & Sun, J. (2017). Zeolite A synthesized from alkaline assisted pre-activated halloysite for efficient heavy metal removal in polluted river water and industrial wastewater. *Journal of environmental sciences*, 56, 254-262.
29. Mthombeni, N. H., Onyango, M. S., & Aoyi, O. (2015). Adsorption of hexavalent chromium onto magnetic natural zeolite-polymer composite. *Journal of the Taiwan Institute of Chemical Engineers*, 50, 242-251.
30. Uzunova, E. L., & Mikosch, H. (2016). Adsorption of phosphates and phosphoric acid in zeolite clinoptilolite: electronic structure study. *Microporous and Mesoporous Materials*, 232, 119-125.
31. Zanin, E., Scapinello, J., de Oliveira, M., Rambo, C. L., Franscescon, F., Freitas, L., ... & Dal Magro, J. (2017). Adsorption of heavy metals from wastewater graphic industry using clinoptilolite zeolite as adsorbent. *Process Safety and Environmental Protection*, 105, 194-200.
32. Castaldi, P., Santona, L., Enzo, S., & Melis, P. (2008). Sorption processes and XRD analysis of a natural zeolite exchanged with Pb<sup>2+</sup>, Cd<sup>2+</sup> and Zn<sup>2+</sup> cations. *Journal of Hazardous Materials*, 156(1-3), 428-434.
33. Elaiopoulos, K., Perraki, T., & Grigoropoulou, E. (2010). Monitoring the effect of hydrothermal treatments on the structure of a natural zeolite through a combined XRD, FTIR, XRF, SEM and N<sub>2</sub>-porosimetry analysis. *Microporous and Mesoporous Materials*, 134(1-3), 29-43.
34. Favvas, E. P., Tsanaktsidis, C. G., Sapalidis, A. A., Tzilantonis, G. T., Papageorgiou, S. K., & Mitropoulos, A. C. (2016). Clinoptilolite, a natural zeolite material: Structural characterization and performance evaluation on its dehydration properties of hydrocarbon-based fuels. *Microporous and Mesoporous Materials*, 225, 385-391.
35. Soyulu, G. S. P., Özçelik, Z., & Boz, İ. (2010). Total oxidation of toluene over metal oxides supported on a natural clinoptilolite-type zeolite. *Chemical Engineering Journal*, 162(1), 380-387.
36. Wang, S., & Peng, Y. (2010). Natural zeolites as effective adsorbents in water and wastewater treatment. *Chemical engineering journal*, 156(1), 11-24.
37. Schick, J., Caullet, P., Paillaud, J. L., Patarin, J., & Mangold-Callarec, C. (2010). Batch-wise nitrate removal from water on a surfactant-modified zeolite. *Microporous and Mesoporous Materials*, 132(3), 395-400.
38. Christidis, G. E., Moraetis, D., Keheyan, E., Akhalbedashvili, L., Kekelidze, N., Gevorkyan, R., ... & Sargsyan, H. (2003). Chemical and thermal modification of natural HEU-type zeolitic materials from Armenia, Georgia and Greece. *Applied Clay Science*, 24(1-2), 79-91.
39. Cakicioglu-Ozkan, F., & Ulku, S. (2005). The effect of HCl treatment on water vapor adsorption characteristics of clinoptilolite rich natural zeolite. *Microporous and Mesoporous Materials*, 77(1), 47-53.
40. Nezamzadeh-Ejehieh, A., & Kabiri-Samani, M. (2013). Effective removal of Ni (II) from aqueous solutions by modification of nano particles of clinoptilolite with dimethylglyoxime. *Journal of Hazardous Materials*, 260, 339-349.

41. Salem, A., & Sene, R. A. (2011). Removal of lead from solution by combination of natural zeolite–kaolin–bentonite as a new low-cost adsorbent. *Chemical engineering journal*, 174(2-3), 619-628.
42. Mudasir, M., Karelius, K., Aprilita, N. H., & Wahyuni, E. T. (2016). Adsorption of mercury (II) on dithizone-immobilized natural zeolite. *Journal of Environmental Chemical Engineering*, 4(2), 1839-1849.
43. Tehrani, R. M. A., & Salari, A. A. (2005). The study of dehumidifying of carbon monoxide and ammonia adsorption by Iranian natural clinoptilolite zeolite. *Applied surface science*, 252(3), 866-870.
44. Ramesh, T. N., Kirana, D. V., Ashwini, A., & Manasa, T. R. (2017). Calcium hydroxide as low cost adsorbent for the effective removal of indigo carmine dye in water. *Journal of Saudi Chemical Society*, 21(2), 165-171.
45. Gollsch, M., Afflerbach, S., Angadi, B. V., & Linder, M. (2020). Investigation of calcium hydroxide powder for thermochemical storage modified with nanostructured flow agents. *Solar Energy*, 201, 810-818.
46. Hlaing, N. N., Vignesh, K., Sreekantan, S., Pung, S. Y., Hinode, H., Kurniawan, W., ... & Salim, C. (2016). Effect of cetyl trimethyl ammonium bromide concentration on structure, morphology and carbon dioxide adsorption capacity of calcium hydroxide based sorbents. *Applied Surface Science*, 363, 586-592.
47. Teimouri, A., Nasab, S. G., Vahdatpoor, N., Habibollahi, S., Salavati, H., & Chermahini, A. N. (2016). Chitosan/Zeolite Y/Nano ZrO<sub>2</sub> nanocomposite as an adsorbent for the removal of nitrate from the aqueous solution. *International journal of biological macromolecules*, 93, 254-266.
48. Widiastuti, N., Wu, H., Ang, M., & Zhang, D. K. (2008). The potential application of natural zeolite for greywater treatment. *Desalination*, 218(1-3), 271-280.
49. Onyango, M. S., Masukume, M., Ochieng, A., & Otieno, F. (2010). Functionalised natural zeolite and its potential for treating drinking water containing excess amount of nitrate. *Water SA*, 36(5).
50. Guan, H., Bestland, E., Zhu, C., Zhu, H., Albertsdottir, D., Hutson, J., ... & Ellis, A. V. (2010). Variation in performance of surfactant loading and resulting nitrate removal among four selected natural zeolites. *Journal of hazardous materials*, 183(1-3), 616-621.
51. Montes-Hernandez, G., Concha-Lozano, N., Renard, F., & Quirico, E. (2009). Removal of oxyanions from synthetic wastewater via carbonation process of calcium hydroxide: Applied and fundamental aspects. *Journal of Hazardous Materials*, 166(2-3), 788-795.
52. Masomboon, N., Chen, C. W., Anotai, J., & Lu, M. C. (2010). A statistical experimental design to determine o-toluidine degradation by the photo-Fenton process. *Chemical Engineering Journal*, 159(1-3), 116-122.
53. Chidambaram, R. (2016). Rice husk as a low cost nanosorbent for 2, 4-dichlorophenoxyacetic acid removal from aqueous solutions. *Ecological Engineering*, 92, 97-105.
54. VAHDAT, P. Z., Asilian, H., & JONIDI, J. A. (2014). Adsorption of xylene from air by natural Iranian zeolite.
55. Daniele, V., Taglieri, G., & Quaresima, R. (2008). The nanolimes in cultural heritage conservation: characterisation and analysis of the carbonatation process. *Journal of cultural heritage*, 9(3), 294-301.
56. Calka, A., & Wexler, D. (2001, January). A study of the evolution of particle size and geometry during ball milling. In *Materials Science Forum* (Vol. 360, pp. 301-310). Trans Tech Publications Ltd.

57. Arbain, R., Othman, M., & Palaniandy, S. (2011). Preparation of iron oxide nanoparticles by mechanical milling. *Minerals Engineering*, 24(1), 1-9.
58. Royae, S. J., Falamaki, C., Sohrabi, M., & Talesh, S. S. A. (2008). A new Langmuir–Hinshelwood mechanism for the methanol to dimethylether dehydration reaction over clinoptilolite-zeolite catalyst. *Applied Catalysis A: General*, 338(1-2), 114-120.
59. Ismail, S., & Khattab, A. (2018). Optimization of proniosomal itraconazole formulation using Box Behken design to enhance oral bioavailability. *Journal of Drug Delivery Science and Technology*, 45, 142-150.
60. Sadoun, O., Rezgui, F., & G'Sell, C. (2018). Optimization of valsartan encapsulation in biodegradables polyesters using Box-Behnken design. *Materials science and engineering: C*, 90, 189-197.
61. Chen, H., & Wang, A. (2007). Kinetic and isothermal studies of lead ion adsorption onto palygorskite clay. *Journal of Colloid and Interface Science*, 307(2), 309-316.
62. Samarghandi, M. R., Al-Musawi, T. J., Mohseni-Bandpi, A., & Zarrabi, M. (2015). Adsorption of cephalixin from aqueous solution using natural zeolite and zeolite coated with manganese oxide nanoparticles. *Journal of molecular liquids*, 211, 431-441.
63. El-Kamash, A. M., Zaki, A. A., & El Geleel, M. A. (2005). Modeling batch kinetics and thermodynamics of zinc and cadmium ions removal from waste solutions using synthetic zeolite A. *Journal of hazardous materials*, 127(1-3), 211-220.
64. Zhan, Y., Lin, J., & Zhu, Z. (2011). Removal of nitrate from aqueous solution using cetylpyridinium bromide (CPB) modified zeolite as adsorbent. *Journal of hazardous materials*, 186(2-3), 1972-1978.
65. Noroozifar, M., Khorasani-Motlagh, M., & Naderpour, H. (2014). Modified nanocrystalline natural zeolite for adsorption of arsenate from wastewater: Isotherm and kinetic studies. *Microporous and Mesoporous Materials*, 197, 101-108.
66. Wibowo, E., Rokhmat, M., & Abdullah, M. (2017). Reduction of seawater salinity by natural zeolite (Clinoptilolite): Adsorption isotherms, thermodynamics and kinetics. *Desalination*, 409, 146-156.
67. Yousef, R. I., El-Eswed, B., & Ala'a, H. (2011). Adsorption characteristics of natural zeolites as solid adsorbents for phenol removal from aqueous solutions: kinetics, mechanism, and thermodynamics studies. *Chemical engineering journal*, 171(3), 1143-1149.
68. Repo, E., Warchol, J. K., Kurniawan, T. A., & Sillanpää, M. E. (2010). Adsorption of Co (II) and Ni (II) by EDTA-and/or DTPA-modified chitosan: kinetic and equilibrium modeling. *Chemical engineering journal*, 161(1-2), 73-82.
69. Han RunPing, H. R., Zhang JingJing, Z. J., Han Pan, H. P., Wang YuanFeng, W. Y., Zhao ZhenHui, Z. Z., & Tang MingSheng, T. M. (2009). Study of equilibrium, kinetic and thermodynamic parameters about methylene blue adsorption onto natural zeolite.
70. Liu, W., Sun, W., Han, Y., Ahmad, M., & Ni, J. (2014). Adsorption of Cu (II) and Cd (II) on titanate nanomaterials synthesized via hydrothermal method under different NaOH concentrations: role of sodium content. *Colloids and Surfaces A: Physicochemical and Engineering Aspects*, 452, 138-147.
71. Kaya, A., & Ören, A. H. (2005). Adsorption of zinc from aqueous solutions to bentonite. *Journal of hazardous materials*, 125(1-3), 183-189.
72. Wang, W., Chen, H., & Wang, A. (2007). Adsorption characteristics of Cd (II) from aqueous solution onto activated palygorskite. *Separation and purification Technology*, 55(2), 157-164.
73. Bhattacharya, A. K., Mandal, S. N., & Das, S. K. (2006). Adsorption of Zn (II) from aqueous solution by using different adsorbents. *Chemical Engineering Journal*, 123(1-2), 43-51.

74. Atar, N., Olgun, A., & Wang, S. (2012). Adsorption of cadmium (II) and zinc (II) on boron enrichment process waste in aqueous solutions: batch and fixed-bed system studies. *Chemical Engineering Journal*, 192, 1-7.
75. Chung, H. K., Kim, W. H., Park, J., Cho, J., Jeong, T. Y., & Park, P. K. (2015). Application of Langmuir and Freundlich isotherms to predict adsorbate removal efficiency or required amount of adsorbent. *Journal of Industrial and Engineering Chemistry*, 28, 241-246.
76. Mittal, A., Kurup, L., & Mittal, J. (2007). Freundlich and Langmuir adsorption isotherms and kinetics for the removal of Tartrazine from aqueous solutions using hen feathers. *Journal of hazardous materials*, 146(1-2), 243-248.
77. Bayramoglu, G., Gursel, I., Tunali, Y., & Arica, M. Y. (2009). Biosorption of phenol and 2-chlorophenol by *Funalia trogii* pellets. *Bioresource technology*, 100(10), 2685-2691.

Article in Press